Applied Catalysis B: Environmental 134–135 (2013) 55–59

Contents lists available at SciVerse ScienceDirect

Applied Catalysis B: Environmental

journal homepage: www.elsevier.com/locate/apcatb

Kinetics of the NO/NO_2 equilibrium reaction over an iron zeolite catalyst

V. Bacher[a], C. Perbandt[b], M. Schwefer[b], R. Siefert[b], T. Turek[a,*]

[a] Institute of Chemical Process Engineering, Clausthal University of Technology, 38678 Clausthal-Zellerfeld, Germany
[b] ThyssenKrupp Uhde GmbH, 44141 Dortmund, Germany

ARTICLE INFO

Article history:
Received 30 July 2012
Received in revised form
21 December 2012
Accepted 29 December 2012
Available online 4 January 2013

Keywords:
NO oxidation
Iron zeolite
Kinetics

ABSTRACT

The steady-state kinetics of NO oxidation and its reverse reaction were studied by systematic measurements in an integral reactor at a range of temperatures, reactor pressures and reactant concentrations on a commercial iron zeolite catalyst. A Langmuir–Hinshelwood type rate equation was found to describe the experimental results with very good accuracy. The reaction orders for NO and O_2 were found to be 1 and 0.75, respectively, while the reaction was inhibited by both NO_2 and H_2O. For the first time, the kinetics developed allow the influence of water vapor on the rate of the NO/NO_2 equilibrium reaction both in the concentration range above and below 1 vol% H_2O to be described.

1. Introduction

Iron exchanged zeolites have received much attention in recent years as catalysts for the removal of nitrogen oxides. A special feature of this catalyst system is its activity for both the reduction of NO_x (NO and NO_2) with ammonia (SCR) [1] and the decomposition and reduction of N_2O [2]. There are first commercial applications in automotive pollution control through SCR and for the simultaneous abatement of nitrous oxide and NO_x in the EnviNOx® process [3]. The EnviNOx® process is a catalytic tail-end exhaust gas system for nitric acid plants that combines SCR of NO_x with either decomposition or reduction of N_2O [4]. Depending on the specific nitric acid technology, removal of the nitrogen oxides takes place at pressures between atmospheric and about 10 bar.

The rate of the SCR reaction over iron zeolites is strongly dependent on the relative amounts of NO and NO_2 with the fastest reaction occurring in the presence of equimolar mixtures [5]. The decomposition of N_2O, on the other hand, is significantly enhanced in the presence of even traces of NO [6,7]. Moreover, the oxidation of NO in diesel engine exhaust gases is highly desirable, as the produced NO_2 is highly reactive toward soot trapped in diesel particulate filters [8,9]. Hence, it is obvious that the oxidation of NO (1) is an important step for a variety of technically important reactions.

$$2\,NO + O_2 \rightleftharpoons 2\,NO_2 \quad (1)$$

The kinetics of NO oxidation over iron-containing zeolites have been studied in a few investigations only. Giles et al. [10] conducted NO oxidation on a Fe-MFI catalyst prepared by solid-state ion exchange. High NO oxidation conversions were achieved at temperatures around 300 °C in the absence of H_2O and SO_2, while both species caused a quite strong inhibition of the reaction rate. Čapek et al. [11] studied NO oxidation using copper and iron exchanged MFI catalysts in the temperature range 200–350 °C. In these experiments, NO oxidation was studied in the absence of water vapor, where a strong inhibition of the reaction rate by the adsorption of NO_2 was observed over both catalyst types. Schuler et al. [12] studied the ammonia SCR on iron zeolite catalysts. In some of their experiments, the NO oxidation was investigated at different NO inlet concentrations in the presence of 5 vol% H_2O at temperatures between 150 and 450 °C. The results were kinetically modeled using the equation developed by Hauptmann et al. [13] for NO oxidation over Pt/Al_2O_3. Sjövall et al. [14] conducted NO oxidation experiments at 150–650 °C in the presence of water vapor (5 vol%) using a commercial washcoated iron zeolite monolith. Markatou et al. [15] studied the NO oxidation over a commercial iron zeolite SCR catalyst under transient and steady-state conditions with gas streams containing 4.5 vol% CO_2 and 4.5 vol% O_2 in the absence of water vapor. Chatterjee et al. [16] did not investigate the NO oxidation individually, however, they have fitted the kinetics of this reaction to SCR experiments on an iron zeolite catalyst in the presence of ammonia. Brüggemann and Keil [17] studied the NO oxidation theoretically over Fe-MFI catalysts. Their results strongly support the experimental findings of Giles et al. [10] and Devadas et al. [5] that water vapor has an inhibiting effect on the rate of NO oxidation. Recently, Metkar et al. [18] have investigated NO oxidation over iron and copper zeolite catalysts. The influence of water was

* Corresponding author. Tel.: +49 5323 722184; fax: +49 5323 722182.
E-mail addresses: bacher@icvt.tu-clausthal.de (V. Bacher), christian.perbandt@thyssenkrupp.com (C. Perbandt), meinhard.schwefer@thyssenkrupp.com (M. Schwefer), rolf.siefert@thyssenkrupp.com (R. Siefert), turek@icvt.tu-clausthal.de (T. Turek).

0926-3373/$ – see front matter © 2013 Elsevier B.V. All rights reserved.
http://dx.doi.org/10.1016/j.apcatb.2012.12.042

studied in the concentration range typical for automotive applications (2–5 vol%). Reaction rates were determined by measurements in a differentially operated tubular reactor and a kinetic model based on elementary steps was developed that included the inhibition of reaction rates by nitrogen dioxide and water vapor.

A deficiency of the existing experimental work on NO oxidation is the limitation to water vapor concentrations above 1 vol%. Consequently, no kinetic model describing the effect of water vapor at low concentrations is available. This is justified by the fact that the reactions relevant for ammonia SCR under automotive exhaust conditions, where high H_2O concentrations are always present, are hardly influenced by the water concentration. However, the catalysts employed in the EnviNOx® process [3,4] for the removal of nitrogen oxides from nitric acid exhaust gases usually encounter much lower water concentrations. This is because the catalyst is located after the adsorption tower, which is operated close to ambient temperature with corresponding low equilibrium water vapor concentrations. Therefore, we have investigated NO oxidation over a commercial iron zeolite catalyst in a broad range of temperatures, pressures and reactant compositions taking into account variations of NO, NO_2, O_2, and H_2O concentrations. The measured data were described with a global Langmuir–Hinshelwood type kinetic model.

2. Experimental

A commercial iron zeolite catalyst (Clariant Süd-Chemie AG, EnviCat®-NOx) was used for the experiments [19]. The catalytic material employed had been exposed to typical reaction temperatures and reactant concentrations in a nitric acid plant exhaust gas stream for 3 months and exhibited stable catalytic properties. The as-received catalyst bodies were crushed and sieved to a 315–500 μm fraction which was packed in an 18 mm stainless steel tube mounted vertically in a cylindrical oven. The packing height for the 6.0 g of catalyst employed amounted to approximately 3.7 cm.

The reactant mixtures (2000 cm^3/min (NTP), down flow) were obtained by feeding NO, NO_2, O_2 and N_2 via electronic mass flow controllers (Bronkhorst High-Tech) from pressurized gas cylinders, while water was dosed by means of a liquid mass flow controller (LIQUI-FLOW, Bronkhorst High-Tech) through a tube into an evaporator system (CEM, Bronkhorst High-Tech). The absolute reactor pressure could be maintained with a regulating valve (HI-TEC, Bronkhorst High-Tech) in the range between 1 and 15 bar. The inlet and outlet reactor streams were analyzed using a FTIR spectrometer (Nicolet 5700, Thermo Scientific), equipped with a 2 m gas cell, as well as a thermomagnetic oxygen analyzer (Oxymat 6, Siemens).

The NO oxidation was studied at temperatures from 200 to 500 °C. The feed contained 200–1000 ppm NO, 0–200 ppm NO_2, 0.2–3.7 vol% O_2 and 0.11–1.07 vol% H_2O balanced in N_2. The total pressure was varied between 1.55 and 6.63 bar. Steady-state conditions were observed after about 15 min, while measurements at increasing and decreasing temperatures yielded identical results.

3. Kinetic model

3.1. Literature models

The NO oxidation kinetics of Hauptmann et al. [13] developed for precious metal catalysts is a power-law equation (2) with reaction orders of 0.28 for NO and 0.49 for O_2, taking the reverse reaction into account via the equilibrium constant (3).

$$r = k_0 \cdot \exp\left(\frac{-E}{R \cdot T}\right) \cdot c_{NO}^{0.28} \cdot c_{O_2}^{0.49} \cdot \left(1 - \frac{c_{NO_2}}{c_{NO} \cdot c_{O_2}^{0.50} \cdot K_{eq}}\right) \quad (2)$$

$$K_{eq} = \frac{c_{NO_2,eq}}{c_{NO_2,eq} \cdot c_{O_2,eq}^{0.50}} \quad (3)$$

This equation was developed for temperatures between 100 and 370 °C, NO feed concentrations from 75 to 450 ppm and a constant O_2 concentration of 6 vol%.

Chatterjee et al. [16] used a similar kinetics with reaction orders of 1 for NO and 0.5 for oxygen Eq. (4 and 5). The parameters are valid for temperatures from 150 to 450 °C and feed concentrations of 500–1000 ppm NO, 2–10 vol% O_2, and 1–10 vol% H_2O.

$$r = k_0 \cdot \exp\left(\frac{-E}{R \cdot T}\right) \cdot \left(c_{NO} \cdot y_{O_2}^{0.5} - \frac{c_{NO_2}}{K_{eq}}\right) \quad (4)$$

$$K_{eq} = \exp\left(\frac{E_{eq}(T)}{R \cdot T}\right) \quad (5)$$

In contrast, Čapek et al. [11] observed an inhibition of the reaction rates by adsorption of NO_2 (6).

$$r = \frac{k_0 \cdot \exp\left(\frac{-E}{R \cdot T}\right) \cdot P_t^3 \left(\frac{y_{NO}^2 \cdot y_{O_2} - y_{NO_2}^2}{P_t \cdot K_{eq}^2}\right)}{\left(1 + K_{NO_2} \cdot P_t \cdot y_{NO_2}\right)^3} \quad (6)$$

Here, y_i is the mole fraction of species i and P_t is the total pressure. Typical reaction mixtures consisted of 1000 ppm NO_x (1000 ppm NO or 800 ppm NO and 200 ppm NO_2) with 6 vol% O_2. Recently, Metkar et al. [18] have developed an elementary step based model for NO oxidation over iron and copper exchanged zeolite catalysts taking into account the adsorption of oxygen, nitrogen dioxide and water vapor. In preliminary investigations, reaction orders of 0.9–1 for NO, 0.55–0.59 for O_2, and 0.42–0.49 for NO_2 were determined. For the case of excess water (at least 2 vol%), the following simplified rate equation (7) was developed, which has a reaction order of −1 with respect to the normalized H_2O concentration:

$$r = \frac{k_0 \cdot \exp\left(\frac{-E}{R \cdot T}\right) \cdot \left(X_{NO} \cdot X_{O_2}^{0.5} - X_{NO_2}/K_{eq}\right)}{X_{H_2O}} \quad (7)$$

During these experiments, different concentrations of NO_x (500 ppm, NO_2/NO_x = 0.25, 0.5 and 0.75), O_2 (5 vol%) and water (2 and 5 vol%) were employed over a range of temperatures (150–550 °C). All cited studies relate to automotive catalysis and were therefore carried out at atmospheric pressure.

3.2. New model

As some of our experimental results, especially at water concentrations below 1 vol% and at higher reactor pressures, could not be described with one of the previously published models, a new kinetic equation had to be developed. This rate equation is of the Langmuir–Hinshelwood type taking into account the inhibition by water vapor and nitrogen dioxide (8)

$$r = \frac{k_0 \cdot \exp\left(\frac{-E}{R \cdot T}\right) \cdot c_{NO} \cdot c_{O_2}^n - \left(\frac{c_{NO_2} \cdot c_{O_2}^{n-0.5}}{K_{eq}^{0.5}}\right)}{\left(1 + K_{NO_2} \cdot c_{NO_2} + K_{H_2O} \cdot c_{H_2O}^m\right)^2} \quad (8)$$

with the equilibrium constant given by:

$$K_{eq} = \frac{c_{NO_2}^2}{c_{NO}^2 \cdot c_{O_2}} \quad (9)$$

The concentration-based equilibrium constant K_{eq} is obtained from the thermodynamic equilibrium constant

$$K^0 = \exp\left(\frac{-\Delta_R G(T,p)}{R \cdot T}\right) \quad (10)$$

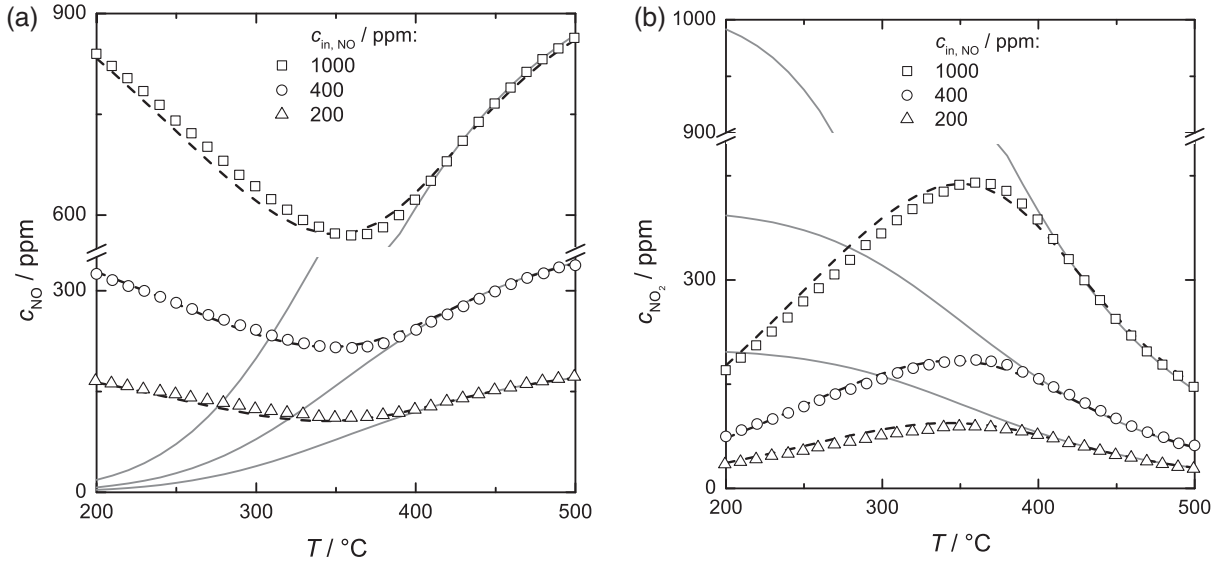

Fig. 1. Measured and calculated NO (left) and NO_2 (right) outlet concentrations as a function of temperature at different NO inlet concentrations (reactor pressure 1.55 bar, 2.5 vol% O_2 and 3200 ppm H_2O at reactor inlet), solid lines: equilibrium, broken lines: simulations.

with the following relationship

$$K_{eq} = K^0 \cdot (R \cdot T)^{-\sum \nu_i} \tag{11}$$

where the change in the number of moles $\Sigma\nu_i$ amounts to −1 according to the stoichiometric equation (1). The thermodynamic data for the calculation of the equilibrium constant (10) were taken from the NIST databank [20].

The laboratory reactor could be regarded as isothermal due to the very small reaction enthalpy. At the given length of the catalytic packing, the Bodenstein number was larger than 100, thus plug flow behavior could be assumed. The kinetic parameters k, E, K_{NO_2}, K_{H_2O} as well as the reaction orders n and m were determined by fitting measured and calculated outlet concentrations in the integral reactor. The simulations were conducted using the software package Presto-Kinetics. Ordinary differential equations were solved applying the MEC (2) solver operating at an accuracy of 10^{-6}. Simulated annealing and box searches were used to obtain starting values for parameter estimations. Optimized values were determined applying a damped Gauss–Newton algorithm [21].

4. Results and discussion

The parameter fit yielded the kinetic parameters summarized in Table 1. The activation energy is in good agreement with Chatterjee et al. [16], while Čapek et al. [11] observed a higher value of 42 kJ/mol. The inhibition constant for NO_2 is of the same order of magnitude as the value of 80 m^3/mol (recalculated with the ideal gas law) given by Čapek et al. [11]. The inhibition of water is not as strong as in the kinetics developed by Metkar et al. [18] with a reaction order of −1.

The possible influence of mass transfer phenomena on the observed reaction rates was estimated by calculation of catalyst effectiveness factors using a simplified first-order approach. The overall effectiveness factor η_{ov}, which is the ratio of observed rate and reaction rate for bulk concentrations, includes both internal and external diffusion limitations. On the other hand, the effectiveness factor η comparing observed rate and reaction rate for catalyst surface concentrations, takes into account pore diffusion only. According to classical theory, the effectiveness factor is a function of the Thiele modulus ϕ (12).

$$\eta = \frac{\tanh(\phi)}{\phi} \tag{12}$$

The Thiele modulus can be expressed with the following equation

$$\phi = L \cdot \sqrt{\frac{k_V}{D_{eff}}} \tag{13}$$

where L is the characteristic diffusion length (assuming one sixth of the equivalent average particle diameter) and k_v the volume specific pseudo first-order rate constant. The intrinsic rate constant k_v was calculated with the apparent mass specific rate constant $k_{m,app}$ which was obtained from the measured NO conversion X_{NO}in the plug-flow reactor, and the apparent density of the catalyst particles ρ_p (1110 kg/m^3):

$$k_V = \frac{k_{m,app} \cdot \rho_p}{\eta} \tag{14}$$

The effective diffusivity was based on a particle porosity of 0.38 and a tortuosity of 2.9 taking into account both Knudsen and binary diffusion coefficients of NO [22]. Thiele modulus and effectiveness factor are then finally calculated iteratively with Eqs. (12)–(14).

For calculation of the overall effectiveness factor, the mass transfer coefficient, which can be obtained from correlations for the Sherwood number, has to be taken into account additionally. The following equation for η_{ov} has been used:

$$\eta_{ov} = \frac{1}{k_v \cdot L/\beta + 1/\eta} \tag{15}$$

The results for the highest NO conversion rate during our measurements are summarized in Table 2.

It can be clearly seen that the calculated catalyst effectiveness factors are very close to 100%. This means that the influence of both, internal and external mass transfer phenomena on the measured reaction rates can be neglected, which is in agreement with Metkar et al. [18].

The results in Fig. 1 show that the equilibrium concentrations of NO and NO_2 are reached at temperatures around 400 °C, with a tendency to higher temperatures at higher nitric oxide inlet concentrations. Experimental and calculated values for both NO and

Table 1
Kinetic parameters of Eq. (8).

k_0	E (kJ/mol)	K_{NO_2} (m^3/mol)	Water inhibition	n_{O_2}
10.35 $m^{5.25}$/kg/s/$mol^{0.75}$	31.0	27.9	$K_{H_2O} = 1.98$ $m^{1.5}$/$mol^{0.5}$ $m_{H_2O} = 0.5$	0.75

Table 2
Calculation of the catalyst effectiveness factors.

T (°C)	X_{NO}	$k_{m,app}$ (m^3/kg/s)	D_{eff} (m^2/s)	L (m)	ϕ	η	β (m/s)	η_{ov}
270	0.86	0.0146	5.00×10^{-6}	6.75×10^{-5}	0.148	0.993	0.57	0.991

NO_2 are in very good agreement. In all measurements, the sum of both nitrogen oxides was equivalent to the inlet concentrations with a deviation of less than 3%. For that reason, only the NO concentrations are depicted in the following diagrams. Fig. 2 reveals that the measured concentrations using a mixture of NO and NO_2 at reactor inlet can also be described with good accuracy.

The effect of oxygen concentration on equilibrium and reaction rate of NO oxidation is shown in Fig. 3. It can be seen that the equilibrium is shifted in the expected way and that the reaction rate is accelerated at rising O_2 concentrations. In contrast to former research, a reaction order of 0.75 with respect to oxygen was found to be most suitable for description of the measured results.

The influence of the H_2O concentration on the rate of NO oxidation is depicted in Fig. 4. During these measurements, the equilibrium conditions remain constant. It is evident that the kinetics are strongly inhibited by water vapor in the concentration range studied. With the new kinetic equation, reaction rates and the resulting reactor outlet concentrations can be described over a range of water vapor concentrations between 0.11 and 1.07 vol%. It must be noted that the rate equation does not hold in the complete absence of water, where the measured NO outlet concentrations are significantly lower than the calculated values (Fig. 4, lower broken line). Attempts to describe the water inhibition with a single reaction order over the whole range of concentrations were not successful. Obviously, the inhibition of reaction rates is very strong

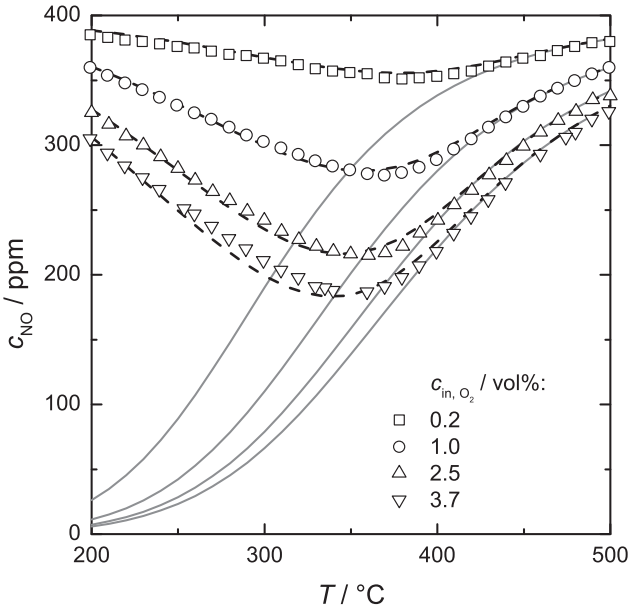

Fig. 3. Effect of oxygen concentration on measured and calculated NO outlet concentrations as a function of temperature (reactor pressure 1.55 bar, 400 ppm NO and 3200 ppm H_2O at reactor inlet), solid lines: equilibrium, broken lines: simulations.

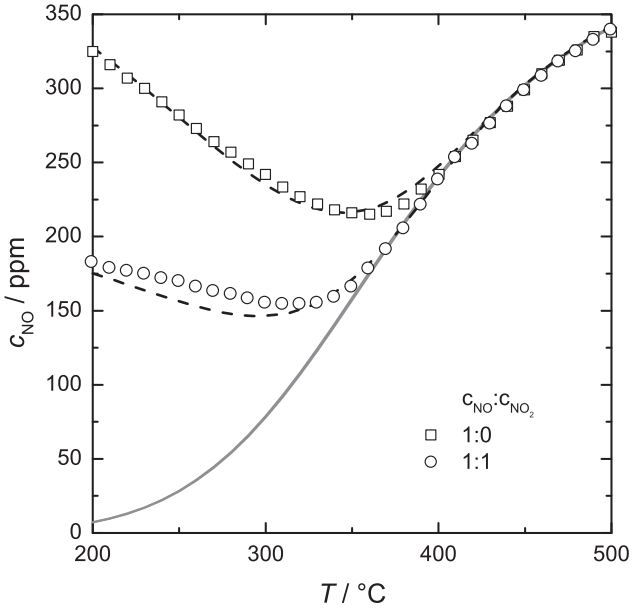

Fig. 2. Measured and calculated NO outlet concentrations as a function of temperature for 400 ppm NO and a mixture of 200 ppm NO and 200 ppm NO_2 at reactor inlet (reactor pressure 1.55 bar, 2.5 vol% O_2 and 3200 ppm H_2O at reactor inlet), solid line: equilibrium, broken lines: simulations.

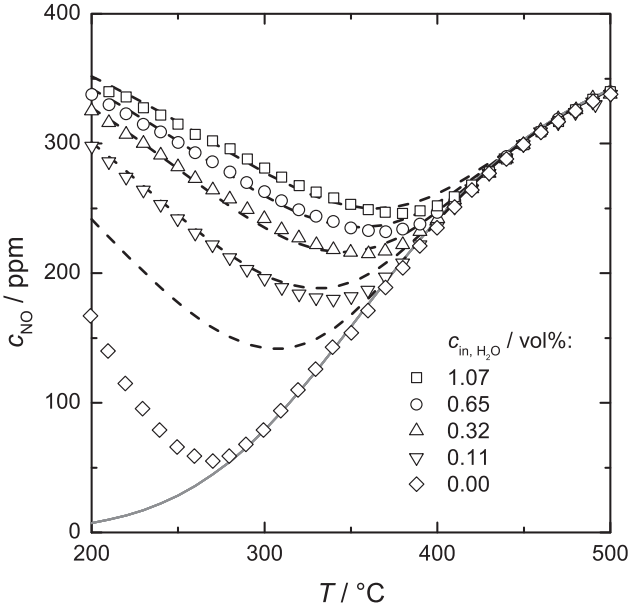

Fig. 4. Measured and calculated NO outlet concentrations as a function of temperature at different H_2O concentrations (reactor pressure 1.55 bar, 2.5 vol% O_2 and 400 ppm NO at reactor inlet), solid line: equilibrium, broken lines: simulations.

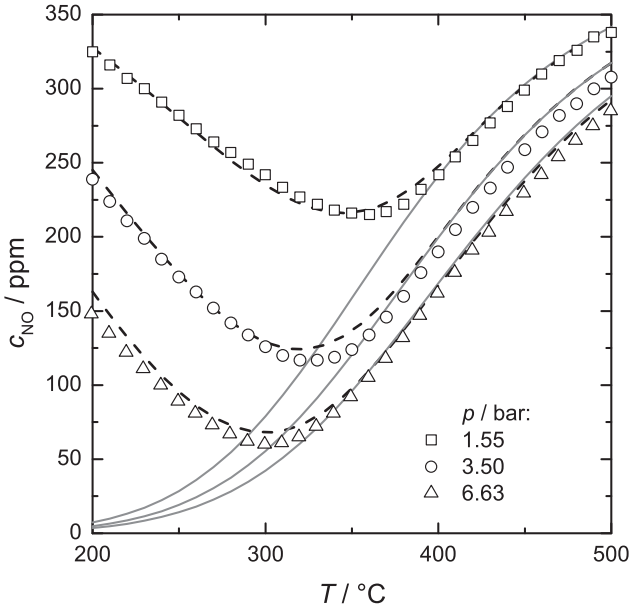

Fig. 5. Effect of total pressure on measured and calculated NO outlet concentrations as a function of temperature (2.5 vol% O_2, 3200 ppm H_2O and 400 ppm NO at reactor inlet), solid lines: equilibrium, broken lines: simulations.

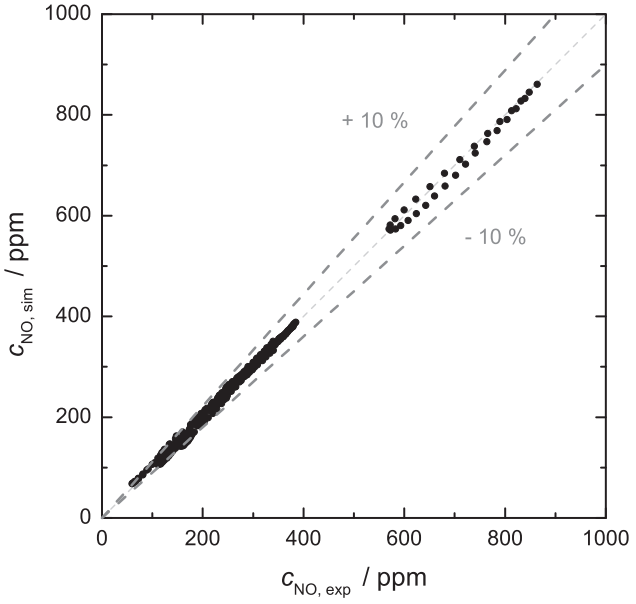

Fig. 6. Parity plot for all measured NO concentration at reactor outlet.

at low water vapor concentrations. However, this phenomenon was not investigated further since all exhaust gases of technical relevance contain a certain water concentration.

Finally, a variation of reactor pressure between 1.55 and 6.63 bar (Fig. 5), during which all concentrations are changed accordingly, shows that the new kinetic equation is appropriate to describe the NO oxidation kinetics over a broad range of temperatures and concentrations. It should be noted that the water concentration of 3200 ppm at a total pressure of 6.63 bar would be equivalent to about 2.1 vol% at atmospheric pressure.

Overall, the present kinetics allow the rate of NO oxidation and the corresponding reverse reaction over a commercial iron zeolite catalyst over a broad range of concentrations to be described with unprecedented accuracy. The parity plot depicted in Fig. 6 reveals that the average standard deviation amounts to only ±2.6%.

5. Conclusions

Systematic measurements of NO oxidation with O_2 and the corresponding reverse reaction were carried out in an integral reactor operated at steady state using a commercial iron zeolite catalyst at different temperatures, concentrations and reactor pressures. The kinetic model developed yielded a very good fit of the experimental data over a broad range of reaction condition. The reaction orders with respect to NO and O_2 were found to be 1 and 0.75, respectively. The reaction rate is inhibited by both NO_2 and H_2O. For the first time, the influence of water vapor on the rate of NO oxidation could be successfully described over a broad concentration range between about 0.1 and 2.1 vol% H_2O.

Acknowledgments

The authors would like to thank Clariant Süd-Chemie AG for kindly providing the catalyst samples.

References

[1] S. Brandenberger, O. Kröcher, A. Tissler, R. Althoff, Catalysis Reviews-Science and Engineering 50 (2008) 492–531.
[2] A. Guzmán-Vargas, G. Delahay, B. Coq, Applied Catalysis B: Environmental 42 (2003) 369–379.
[3] M. Groves, M. Schwefer, R. Siefert, TCE (2006) 30–31.
[4] M.C.E. Groves, A. Sasonov, Journal of Integrative Environmental Sciences 7 (2010) 211–222.
[5] M. Devadas, O. Kröcher, M. Elsener, A. Wokaun, N. Söger, M. Pfeifer, Y. Demel, L. Mussmann, Applied Catalysis B: Environmental 67 (2006) 187–196.
[6] M. Kögel, B.M. Abu-Zied, M. Schwefer, T. Turek, Catalysis Communication 2 (2001) 273–276.
[7] J. Pérez-Ramírez, F. Kapteijn, G. Mul, J.A. Moulijn, Journal of Catalysis 208 (2002) 211–223.
[8] A. Setiabudi, M. Makkee, J.A. Moulijn, Applied Catalysis B: Environmental 50 (2004) 185–194.
[9] B.R. Stanmore, V. Tschamber, J.F. Brilhac, Fuel 87 (2008) 131–146.
[10] R. Giles, N.W. Cant, M. Kögel, T. Turek, D.L. Trimm, Applied Catalysis B: Environmental 25 (2000) L75–L81.
[11] L. Čapek, L. Vradman, P. Sazama, M. Herskovitz, B. Wichterlová, R. Zukerman, R. Brosius, J.A. Martens, Applied Catalysis B: Environmental 70 (2007) 53–57.
[12] A. Schuler, M. Votsmeier, P. Kiwic, J. Gieshoff, W. Hauptmann, A. Drochner, H. Vogel, Chemical Engineering Journal 154 (2009) 333–340.
[13] W. Hauptmann, A. Drochner, H. Vogel, M. Votsmeier, J. Gieshoff, Topics in Catalysis 42-43 (2007) 157–160.
[14] H. Sjövall, R.J. Blint, A. Gopinath, L. Olsson, Industrial & Engineering Chemistry Research 49 (2010) 39–52.
[15] P. Markatou, J. Dai, A. Johansson, W. Klink, M. Castagnola, T.C. Watling, M. Tutuianu, SAE Technical Paper 2011-01-1304.
[16] D. Chatterjee, T. Burkhardt, M. Weibel, I. Nova, A. Grossale, E. Tronconi, SAE Technical Paper 2007-01-1136.
[17] T.C. Brüggemann, F.J. Keil, Journal of Physical Chemistry C 115 (2011) 2114–2133.
[18] P.S. Metkar, V. Balakotaiah, M.P. Harold, Catalysis Today 184 (2012) 115–128.
[19] A. Tissler, T. Turek, M. Kögel, W. Schwieger, M. Rauscher, R. Mönnig, K. Kesore, European Patent EP 0955080 (B1), 1999.
[20] http://www.nist.gov/index.html (retrieved 15.04.09).
[21] M. Wulkow, Handbook Presto-Kinetics, Computing in Technology GmbH, Rastede, 2005.
[22] C. Perbandt, Kinetische Modellierung der Zersetzung von N_2O an Eisen-Zeolith-Katalysatoren in Abgasen der Salpetersäureproduktion, Dissertation, Clausthal University of Technology, 2011.